

# Fabrication of biomimetic placental barrier structures within a microfluidic device utilizing two-photon polymerization

Denise Mandt<sup>1,2</sup>, Peter Gruber<sup>1,2</sup>, Marica Markovic<sup>1,2</sup>, Maximillian Tromayer<sup>2,3</sup>, Mario Rothbauer<sup>3</sup>, Sebastian Rudi Adam Kratz<sup>3</sup>, Syed Faheem Ali<sup>3</sup>, Jasper Van Hoorick<sup>4,5</sup>, Wolfgang Holnthoner<sup>2,6</sup>, Severin Mühleder<sup>2,6</sup>, Peter Dubruel<sup>4</sup>, Sandra Van Vlierberghe<sup>4,5</sup>, Peter Ertl<sup>2,3</sup>, Robert Liska<sup>2,3</sup>, Aleksandr Ovsianikov<sup>1,2\*</sup>

<sup>1</sup> Institute of Materials Science and Technology, TU Wien, Vienna Austria

<sup>2</sup> Austrian Cluster for Tissue Regeneration, Austria

<sup>3</sup> Institute of Applied Synthetic Chemistry, TU Wien, Vienna Austria

<sup>4</sup> Polymer Chemistry and Biomaterials Group, Centre of Macromolecular Chemistry, Ghent University, Ghent, Belgium

<sup>5</sup> Brussels Photonics, Department of Applied Physics and Photonics, Vrije Universiteit Brussel, Brussels, Belgium

<sup>6</sup> Ludwig Boltzmann Institute of Experimental and Clinical Traumatology, Vienna, Austria

**Abstract:** The placenta is a transient organ, essential for development and survival of the unborn fetus. It interfaces the body of the pregnant woman with the unborn child and secures transport of endogenous and exogenous substances. Maternal and fetal blood are thereby separated at any time, by the so-called placental barrier. Current *in vitro* approaches fail to model this multifaceted structure, therefore research in the field of placental biology is particularly challenging. The present study aimed at establishing a novel model, simulating placental transport and its implications on development, in a versatile but reproducible way. The basal membrane was replicated using a gelatin-based material, closely mimicking the composition and properties of the natural extracellular matrix. The microstructure was produced by using a high-resolution 3D printing method – the two-photon polymerization (2PP). In order to structure gelatin by 2PP, its primary amines and carboxylic acids are modified with methacrylamides and methacrylates (GelMOD-AEMA), respectively. High-resolution structures in the range of a few micrometers were produced within the intersection of a customized microfluidic device, separating the x-shaped chamber into two isolated cell culture compartments. Human umbilical-vein endothelial cells (HUVEC) seeded on one side of this membrane simulate the fetal compartment while human choriocarcinoma cells, isolated from placental tissue (BeWo B30) mimic the maternal syncytium. This barrier model in combination with native flow profiles can be used to mimic the microenvironment of the placenta, investigating different pharmaceutical, clinical and biological scenarios. As proof-of-principle, this bioengineered placental barrier was used for the investigation of transcellular transport processes. While high molecular weight substances did not permeate, smaller molecules in the size of glucose were able to diffuse through the barrier in a time-dependent manner. We envision to apply this bioengineered placental barrier for pathophysiological research, where altered nutrient transport is associated with health risks for the fetus.

**Keywords:** high resolution 3D printing; placental barrier; model; microstructure; two-photon polymerization

\*Correspondence to: Aleksandr Ovsianikov, Institute of Materials Science and Technology, TU Wien, Getreidemarkt 9, 1060 Vienna, Austria; [aleksandr.ovsianikov@tuwien.ac.at](mailto:aleksandr.ovsianikov@tuwien.ac.at) (ORCID: 0000-0001-5846-0198)

**Received:** May 14, 2018; **Accepted:** June 18, 2018; **Published Online:** July 3, 2018

**Citation:** Mandt D, Gruber P, Markovic M, 2018, Fabrication of biomimetic placental barrier structures within a microfluidic device utilizing two-photon polymerization. *Int J Bioprint*, 4(2): 144. <http://dx.doi.org/10.18063/IJB.v4i2.144>

Fabrication of biomimetic placental barrier structures within a microfluidic device utilizing two-photon polymerization. © 2018 Mandt D, *et al.* This is an Open Access article distributed under the terms of the Creative Commons Attribution-NonCommercial 4.0 International License (<http://creativecommons.org/licenses/by-nc/4.0/>), permitting all non-commercial use, distribution, and reproduction in any medium, provided the original work is properly cited.

## 1. Introduction

Research, in the field of placental biology, represents a challenging topic. Although a variety of *in vivo* animal models, *ex vivo* placental perfusion models and *in vitro* models have been described, current approaches are difficult to perform, time-consuming and often carry the risk of harming the unborn fetus<sup>[1]</sup>. However, progressive research and the increasing provision of human tissue samples for study purpose enable the advancement of current methods and the establishment of new approaches. In recent years, microfluidic methods have gained increasing attention in this respect<sup>[2]</sup>. This novel and highly interdisciplinary research field combines microfabrication with bioengineering and material sciences. Microfluidic barrier models are of particular interest, as the culture conditions resemble the dynamics similar to native human tissue. The complexity of highly specialized organs, such as, for example the placenta, can be recapitulated using these micro-engineered cell culture systems<sup>[3]</sup> thereby allowing human cells to grow under physiologically relevant conditions<sup>[4]</sup>. With respect to placental biology, this controllable microenvironment can be engineered to reflect the multi-layered membranous structure of the placenta in combination with native conditions, regarding media flow and media composition<sup>[3]</sup>. With a high-resolution 3D-printing technique, the membranous structure of the placental membrane can be mimicked precisely. To simulate the barrier function of the placenta, aside from selection of cell model also the influence of the membrane material has to be considered. A promising material in this context is for instance gelatin, as it is derived from collagen, which is the main component of placental connective tissue, extensively used in tissue engineering<sup>[5,6]</sup>. The main benefit of gelatin is that it can be modified to enhance functionality and versatility of the biomaterial. For instance, the incorporation of methacrylamide groups onto the amine-containing side groups results in a biopolymer (GelMOD), which can be used for photo-crosslinking processes at room temperature<sup>[7]</sup> with high stability at 37 °C after polymerization<sup>[7-9]</sup>.

In addition, the mechanical properties of the material can be improved further by modifying GelMOD with additional methacrylates (GelMOD-AEMA), thereby creating more functional groups for the cross-linking process, which outperforms the mechanical properties of GelMOD and performs better in aqueous environment<sup>[10]</sup>.

Over the last decades, the ongoing trend of miniaturization and multiplexing tissue engineering entails new demands on manufacturing techniques as well as biomaterial compositions and functionalities, especially regarding micrometer-scale resolution. To achieve sub-micrometer spatial resolution a 3D printing technique called two-photon polymerization (2PP) can be

used. This technique takes advantage of two-photon absorption, which results in true 3D structuring and spatial resolution below 100 nm<sup>[8,11,12]</sup>. Due to this very high resolution, structural parameters such as external shape, pore size and internal porosity of fabricated structures can be manufactured in a precise manner<sup>[8,13]</sup>. In this study, GelMOD-AEMA was combined with 2PP to produce high-resolution structures with micrometer-precision, to closely mimic the native microenvironment of placental tissue, as there are currently no publications about utilizing 2PP techniques for fabrication of placental barrier models. Firstly, cellular response of the GelMOD-AEMA biomaterial as well as the applied photoinitiators was tested in a two-dimensional approach to ensure maximal biocompatibility. Secondly, a study on biomaterial composition was performed to find the best-suited, photosensitive material compatible with placental trophoblast cells. Because the establishment of a placenta-on-a-chip model to recreate an *in vivo*-like villous membrane structure was envisaged, resolution and stability of the GelMOD-AEMA 2PP processing were further evaluated. Finally, as proof-of-principle the presented villous placental membrane model was used to study the transport of glucose-sized molecules.

## 2. Experimental

### 2.1 Cell Culture

For this study, human umbilical-vein endothelial cells (HUVEC) and human choriocarcinoma cells (BeWo B30) were grown in 75 cm<sup>2</sup> cell culture flasks (Greiner) as monolayer cultures at 5% CO<sub>2</sub> and 37 °C. Cells were sub-cultivated before reaching confluence, using 1-fold trypsin-EDTA (Sigma) solution. BeWo B30 cells were grown in DMEM Ham nutrient composition F12 media (Sigma) supplemented with 10% fetal bovine serum (FBS - Lonza) and antibiotics (10,000 units/mL penicillin and 10 mg/mL streptomycin in 0.9% sodium chloride, Sigma Aldrich). HUVECs were maintained in supplemented endothelial growth media (EGM2, Lonza) including 2% FBS, 0.04% hydrocortisone, 0.4% human fibroblastic growth factor (hFGF), 0.1% vascular endothelial growth factor (VEGF), 0.1% long-insulin-like growth factor-1 (R3-IGF-1), 0.1% ascorbic acid, 0.1% human endothelial growth factor (hEGF), 0.1% heparin and a mixture of 30 mg/mL gentamicin and 15 µg/mL amphotericin.

### 2.2 Evaluation of Membrane Material Biocompatibility

To evaluate the biocompatibility of the structure material cellular response of seeded HUVECs and BeWo B30 cells was evaluated in a two-dimensional setting. The material under investigation was a 15 wt% GelMOD-AEMA solution containing 0.6 mM of UV sensitive

photoinitiator lithium-(2,4,6-trimethylbenzoyl)-phenylphosphinate (Li-TPO-L), which was synthesized as previously published<sup>[14]</sup>. GelMOD-AEMA surfaces were prepared by applying drops of 50  $\mu$ L warm gel solution on a pre-heated Teflon plate (40 °C). Previously methacrylated cover glasses were carefully placed on top of the droplets and gently pushed against the Teflon plate, in order to guarantee a uniform coating. The Teflon plate with the coverslips was transferred into the UV chamber and exposed to UV light for 10 min at 365 nm, which corresponds to 4 mW/cm<sup>2</sup>. In the meantime, wells of a 12-well cell culture plate were coated with 1% agarose solution dissolved in PBS. Uncoated glasses and glasses covered with a thin layer of GelMOD-AEMA were gently embedded, while the agarose was still warm. Coating the wells with agarose prior to placing the glass slide ensures that cells exclusively stay on the glass and not around or under the glass. Subsequently, unpolymerized material was removed by washing with the respective cell culture media. Samples evaluating the effect of fibronectin-coated GelMOD-AEMA were subsequently incubated with 50  $\mu$ L/mL fibronectin for 30 min, at 37 °C.  $20 \times 10^4$  HUVECs or BeWo B30 cells in 1 mL of the respective cell culture media were seeded per well and allowed to attach overnight.

Determination of metabolic activity was performed 24 and 48 hours post seeding using a resazurin-based staining solution. Cells were incubated for 90 min at 37 °C with 100  $\mu$ L Presto Blue<sup>®</sup> (ThermoFisher) solution which was prepared according to the manufacturer's protocol. For absorbance readout, 100  $\mu$ L supernatant was transferred to a 96-well plate and analyzed with a microplate reader (BioTek Instruments) using an excitation/emission filter of 570 nm and 600 nm, respectively. Furthermore, absolute DNA content was quantified 48 hours' post seeding using the blue fluorometric double-stranded DNA quantification kit FluoReporter<sup>®</sup> (Molecular Probes).

To evaluate changes in cell metabolism and DNA content of cells cultured in co-culture media, HUVECs and BeWo B30 cells were seeded in 12-well plates with an average concentration of  $8 \times 10^4$  cells per well. To compare changes in growth, both cell types, HUVEC and BeWo B30, were either cultured in their supplemented culture media EGM-2 and DMEM Ham F-12, respectively, or cultivated in a 1:1 mixture of these cell media. Changes in metabolic activity and DNA content were evaluated as described above.

### 2.3 Functionalization of Glass Surfaces with Methacrylate Groups

For silanization 18 mm cover glasses (Carl Roth) loaded in appropriate staining racks were pre-treated in a plasma cleaner (Harrick Plasma) for 10 min. The

methacrylization solution consisting of deionized water (50% v/v), ethanol (48% v/v), glacial acetic acid (0.3% v/v) and 3-(trimethoxysilyl)-propyl methacrylate (2% v/v) was prepared under continuous stirring. After a contact time of 30 min, supernatant liquid was removed and coated glasses were washed with deionized-water twice. After drying in a heating cabinet, slides were UV sterilized.

### 2.4 Fabrication of Microfluidic Devices

The complexity of the placental structure and the central requirement of two separately perfusable channels placed special demands on the chip geometry. Therefore, in this study a custom-made microfluidic platform was used.

The chip had a rectangular footprint with dimensions of 76  $\times$  26 mm and two adjacent chambers. Each chamber had four in-/outlets at its outermost points (Figure 1A). The molds of these chambers were X-shaped with an intersection area of 1.4 by 1.0 mm creating an appropriate structure area. (Figure 1B). For chip fabrication poly-(ethylene glycol)-dimethacrylate (PEGdma - Sigma Aldrich) with an average molecular weight of 700 was used. The photosensitive material solution, consisting of 40% v/v polymer solution, 0.6 mM Li-TPO-L photoinitiator and Dulbecco's phosphate buffered saline (DPBS - Sigma) was casted between a prepared glass chip. This chip was composed of three different layers: a 1 mm thick cover glass (Carl Roth) with four orifices, a 250  $\mu$ m polydimethylsiloxane (PDMS) spacer and a 170  $\mu$ m thin bottom glass (ibidi). After chip frames were silanized with methacrylates, the injected PEGdma solution was irradiated for 50 seconds with an UV-LED (OmniCure) at 365 nm. After removal of unpolymerized material, female luer lock connectors (ibidi) were glued on the orifices of the cover glass and the chip was sterilized by UV irradiation. All described fabrication steps were performed under sterile conditions inside a lamina flow hood.

### 2.5 Preparation of the Placental Barrier Model Devices

3D structures were produced within the sterile microfluidic chip using an in-house built 2PP system (SI Figure 1) with a laser pulse length of 70 fs and a repetition rate of 80 MHz at 800 nm (MaiTai, Spectra-Physics). The system is similar to the one reported previously<sup>[15]</sup>. Due to the nonlinear behavior of 2PP, two-photon absorption triggers a local photopolymerization, with a feature size of less than 100 nm<sup>[15]</sup>.

The laser beam was focused into the sample using a 10x microscope objective, and scanned with a velocity of 1 m/s and a laser power of 130 mW. Microfluidic barrier structures were produced in the intersection of

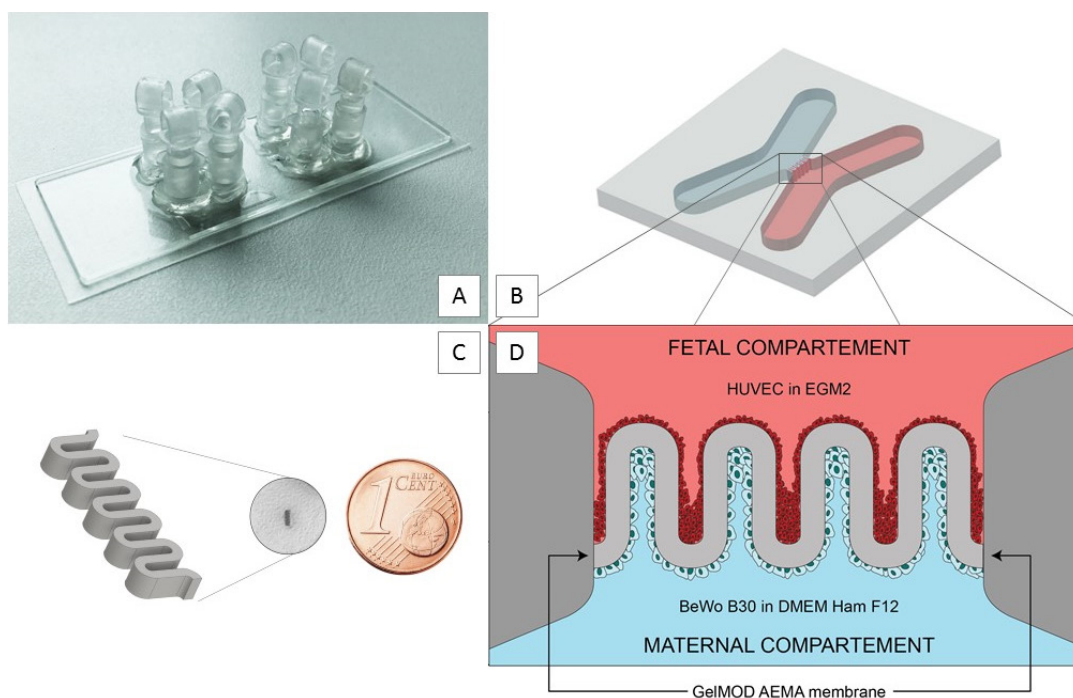


**Figure 1.** Placental barrier within a custom-made microfluidic device with two culture chambers. (A) The assembled microfluidic chip with two placental barrier models per slide. (B) The enlarged intersection of the x-shape geometry containing the 3D printed membrane. (C) The CAD-model of the membrane with five consecutive loops mimics the geometry of the placental barrier. To illustrate the size, the structure is shown next to a 1-eurocent coin. (D) After 2PP structuring, the hydrogel membrane separated the chip into two separately perfusable compartments. The fetal and maternal compartment, which were seeded with HUVECs and BeWo B30 cells, respectively. Cells were cultured under constant flow.

the x-shaped microfluidic chip, separating it into two channels which can be perfused independently (Figure 1B). Thereby, the four ports offer the possibility to culture two distinct cell types under different conditions. The membrane design used in this study is a simplified replication of the villous shape of the placental barrier and therefore consists of five consecutive loops. For structuring, GelMOD-AEMA was dissolved in PBS to a final concentration of 15 wt% and supplemented with 1 mM photoinitiator P2CK<sup>[10]</sup>.

The membrane with 100  $\mu\text{m}$  wall thickness was fabricated directly within the chip. To give an impression of the actual size of the produced structure, it is depicted next to a 1-eurocent coin in Figure 1C. Unpolymerized material was removed after printing by consecutive washing with PBS. The produced membranes were characterized and further used for cell-based experiments. For the placenta-on-a-chip model the membrane was coated with fibronectin. Two different cell types, one for either side, were successively seeded onto the membrane walls. HUVECs and BeWo B30 cells were used to mimic the fetal and maternal compartment, respectively. The initial seeding concentration was calculated at 20,000 cells per chamber, in order to reach

confluence within 7 days. Cells were cultivated in their intended cell culture media under constant flow of 50–70  $\mu\text{L/h}$ . A schematic configuration is shown in Figure 1D.

## 2.6 Evaluation of Hydrogel Membrane Permeability

The semi-permeability of the membrane is a prerequisite for a placenta model. The aim was to structure a membrane which cuts-off large biological molecules ( $> 1$  kDa). Therefore, different molecular weight fluorescence molecules were added to one of the microfluidic channels. Fluorescence images provided information about the membrane permeability and the transportation rate. Those images were subsequently analyzed with paint.net and the ZEN Software. To show the impermeability of the membrane towards large substances, 1 mg/mL fluorescein isothiocyanate dextran (FITC-Dextran – Sigma-Aldrich), with a molecular weight of 200 kDa, was dissolved in DPBS and added to one of the channels. Riboflavin 5'-monophosphate (Riboflavin-350 Da) served as second test compound, showing the permeability to sugar-sized molecules. Riboflavin 5'-Monophosphate sodium salt (TCI) was



dissolved in DPBS to get a final concentration of 1 mg/mL. The diffusion rate was evaluated by taking images at different time points, evaluating the increase in signal intensity over time.

## 2.7 Data Analysis

All statistical calculations were performed with GraphPad Prism 4.0 using the one-way ANOVA with Tukey-Kramer post testing. The probability of error was presented as mean with +/- standard deviation. Determined P-values less than 0.05 were considered as significant and marked in the respective diagram with black asterisks. Error probability was indicated for 5% (\*), less than 1% (\*\*) and less than 0.1% (\*\*\*).

## 3. Results

### 3.1 Fibronectin Supports Attachment of HUVECs and BeWo B30 Cells on GelMOD-AEMA

To verify the biocompatibility of the membrane material, HUVECs and BeWo B30 cells were seeded on UV-polymerized GelMOD-AEMA layers in order to evaluate the effect on cellular behavior. Figure 2 summarizes the results from four independent samples, showing the influence of different substrate materials and coatings on the metabolic activity of HUVEC

(red) and BeWo B30 (blue) cells 24 and 48 hours post seeding. HUVECs cultured on GelMOD-AEMA show the lowest metabolic activity after 24 hours, whereas glass, the fibronectin control as well as the fibronectin-coated GelMOD-AEMA are within the same range. Two days after seeding, metabolic activity of cells cultured on GelMOD-AEMA and fibronectin-coated GelMOD-AEMA exceeded control values. Values obtained from BeWo B30 samples were comparable on both days. GelMOD-AEMA samples show the lowest activity on both days. Quantitative evaluation of DNA content (SI Figure 3) demonstrated that the overall amount of DNA is significantly higher in BeWo B30 samples, compared to HUVEC. Nevertheless, these findings are in line with the changes in metabolic activity, as the highest DNA content was measured in samples cultivated on fibronectin-coated GelMOD-AEMA. Results of BeWo B30 samples also follow this trend. Fibronectin-coated samples exhibited higher DNA content compared to control groups and cells cultivated on GelMOD-AEMA. Overall, these results indicate that by post-treating GelMOD-AEMA with fibronectin, cell survival could be significantly improved.

### 3.2 Co-culture Media does not Negatively Influence Cell Growth

The influence of the co-culture media was analyzed in order to evaluate the effect of possible media mixing

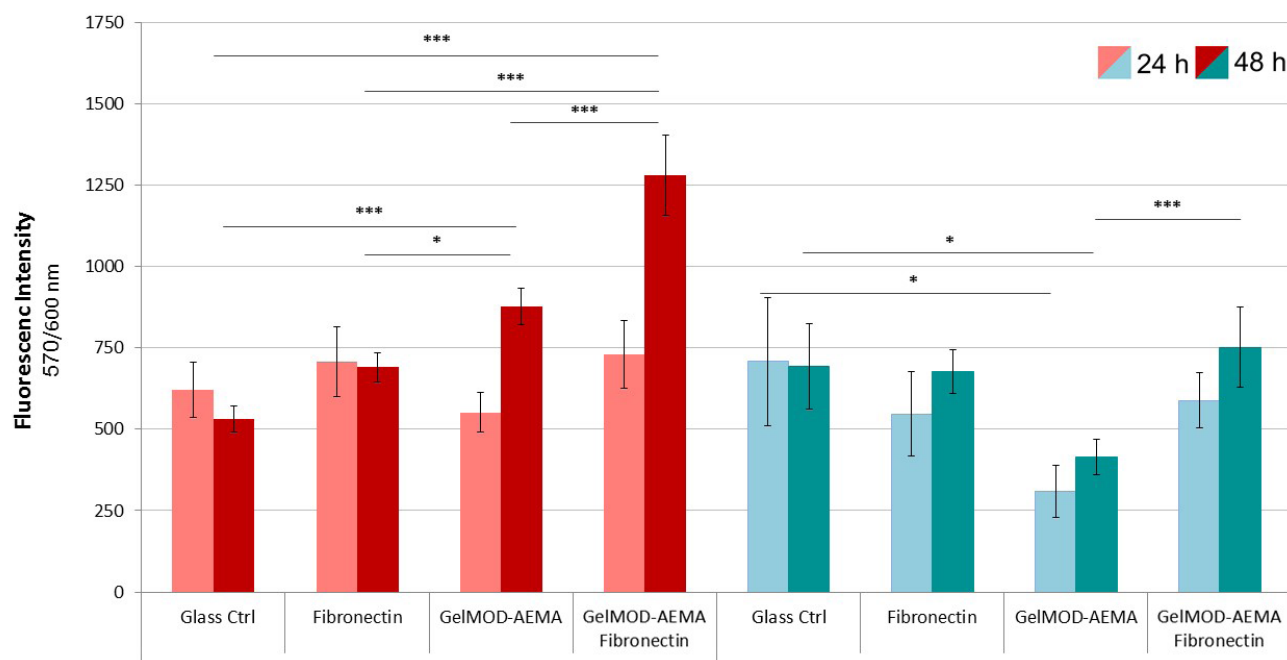


**Figure 2.** Metabolic activity of HUVECs and BeWo B30 cells cultured on different substrates 24 and 48 hours post seeding. This diagram summarizes results from four independent samples, showing the influence of different substrate materials on the metabolic activity of HUVEC (red) and BeWo B30 (blue) cells 24 and 48 hours post seeding.

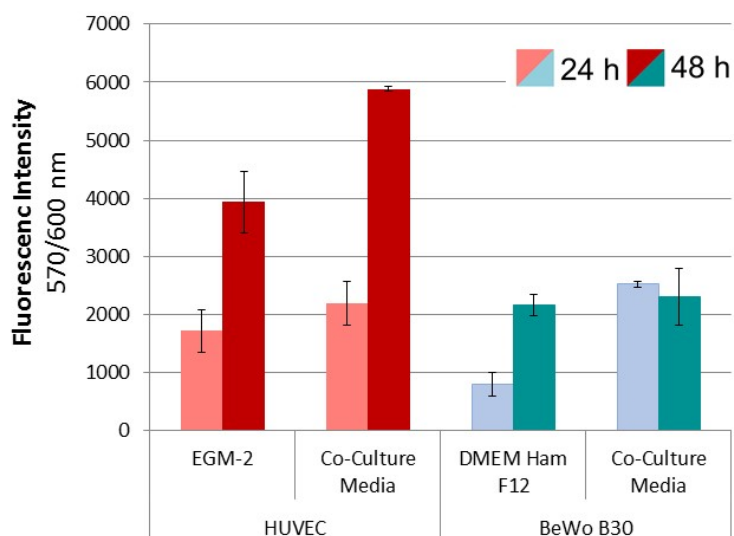


**Figure 3.** Influence of co-culture media on the metabolic activity of both cell types 24 and 48 hours after seeding. The metabolic activity of both cell types was evaluated 24 and 48 hours after seeding. Values obtained from four independent samples served as a basis for the calculations. Samples under investigation included HUVECs (red) and BeWo B30 cells (blue) seeded in their intended cell culture media and co-culture media, respectively.

at the transition zone, as media components of the respective other media can diffuse across the barrier structure, thus influencing the cell proliferation. The influence on cell metabolism (Figure 3) of both cell types, HUVEC and BeWo B30 was evaluated after cells were seeded in co-culture media or their respective cell culture media, resulting in four different samples. Evaluation of metabolic activity showed that co-culture media improves cell activity after 24 as well as after 48 hours of incubation, compared to standard EGM-2 media. Metabolic activity of BeWo B30 cells cultured in their intended cell culture media is comparable to the behavior of HUVECs cultured in EGM-2. Nevertheless, no significant increase in metabolic activity could be observed in samples cultured in co-culture media. DNA-content of HUVECs cultured in co-culture media exceeded those of cells cultured in their intended media. In BeWo B30 samples DNA-content was independent of the culture media, as shown in Figure 2 of the supplementary information.

### 3.3 Determination of 2PP-processing Parameters for Membrane Material

Confocal image analysis of 2PP structures showed that the detected fluorescence signal increases for the structures produced at higher laser intensity. This observation is in line with higher hydrogel crosslinking density, resulting in trapping of more fluorescent P2CK and thus a stronger signal. In a qualitative analysis, fluorescence intensity of structures produced at laser powers between 95 mW and 140 mW, with 5 mW increments were assessed. As shown in Figure 4A, all

tested laser intensities resulted in detectable and stable geometries. To produce long-term stable and complex structures, like a placental barrier, 130 mW was used for printing, as a laser power exceeding 130 mW resulted in local decomposition of the chip material.

In Figure 4B, a  $6 \times 9$  test array produced with 130 mW is shown. During the structuring process, the layer distance ( $dz$ ) was varied from 0.8 to 1.6  $\mu\text{m}$ , whereas the line distance (hatch) was changed from 0.3  $\mu\text{m}$  to 0.8  $\mu\text{m}$ . The variation of  $dz$  does not have a huge influence on the structure stability. Nevertheless, the lowest tested  $dz$  of 0.8  $\mu\text{m}$  was chosen in order to ensure dense crosslinking and thus a small mesh size of the membrane. However, hatch distances exceeding 0.5  $\mu\text{m}$  resulted in a detectable loss of stability. Therefore, 0.4  $\mu\text{m}$  line distance was used.

### 3.4 Semi-permeable Membrane Allows Selective Transport

As the placental membrane is a semi-permeable tissue, the *in vitro* model has to mimic this property. The semi-permeability of structured membranes was demonstrated using two fluorescence-labeled substances differing in molecular weight. Water-soluble dextran with a molecular weight of 200 kDa was used to prove the structures impermeability to large molecules. Riboflavin with 350 Da showed that sugar-sized molecules can diffuse through the membrane. Images of printed structures after development as well as after injection of the dye solution are shown in Figure 5. The first column of Figure 5A shows the fluorescence of the printed membranes without staining. By injecting riboflavin and

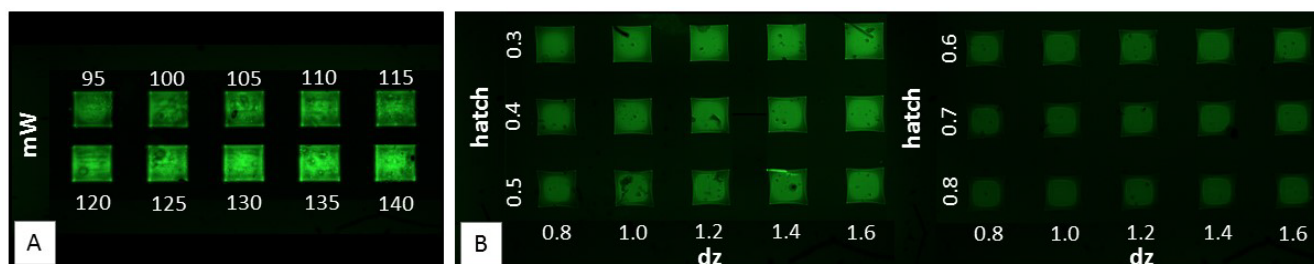


**Figure 4.** Influence of different laser intensity and structuring parameter on structure stability. (A) A  $4 \times 2$  array with laser intensities between 95 and 140 mW was structured and the detected fluorescence intensity was used as parameter for the assessment of standard structure quality. (B) In the second step, the structure quality in dependency on varying hatch and dz values (indicated in  $\mu\text{m}$ ) was

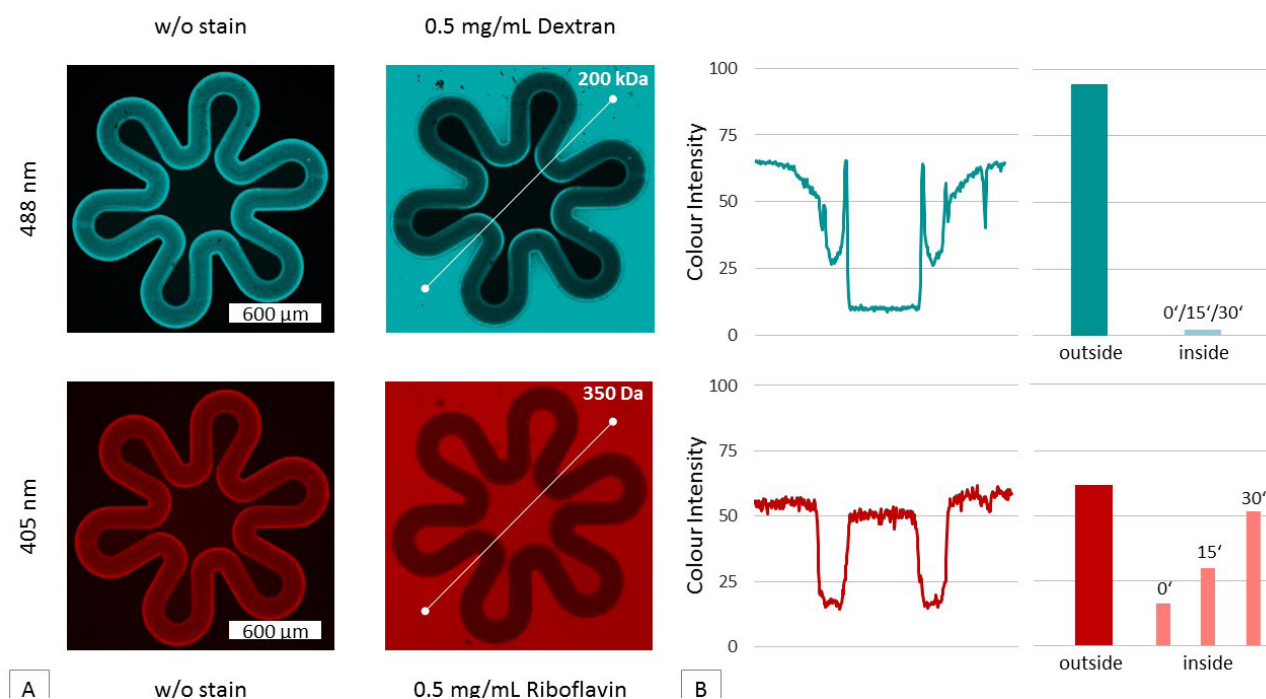


**Figure 5.** Test of semi-permeability of a  $100 \mu\text{m}$  thick hydrogel membrane produced with 2PP techniques. (A) In the first column, fluorescence images taken at different wavelengths (488 and 405 nm filter) highlighting the auto-fluorescence of the membranes are shown. In the second column, fluorescence images taken after injection of the stain solutions are shown. The permeability to sugar-sized molecules and impermeability to larger molecules is demonstrated using a 0.5 mg/mL riboflavin and 0.5 mg/mL dextran solution. (B) Furthermore, the fluorescence intensity was evaluated along the cross-section of the membrane (white line detail A). Thereby arbitrary units (AU) were measured and plotted using ZEN software. In dextran samples, the inner fluorescence signal is approaching zero. Riboflavin (red) intensity on the other side is equal within and outside the villous structure.

dextran, it can be seen that the produced membranes are highly permeable to small molecules, while larger molecules are retained. The fluorescence signal over the cross section of a structure is depicted in in [Figure 5B](#), illustrating the changes in fluorescence signal from outer to inner region as well as in the transition zone. The fluorescent signal of riboflavin within the structure was monitored over a period of 90 min to illustrate the diffusion rate and thus the signal increase over time. The equilibrium of measured fluorescence was achieved after time point three, 30 min after injection.

### 3.5 Membrane Permeability Is Independent of Wall Thickness

The thickness of the placental membrane changes during the course of pregnancy<sup>[16]</sup>. Therefore, another factor under investigation, which potentially influences the membrane permeability, was wall thickness. To investigate this, the fluorescence evaluation was repeated with a villous geometry where the wall thickness was reduced to  $25 \mu\text{m}$ . [Figure 6](#) shows that, similar to the first experiment, riboflavin was detectable on both

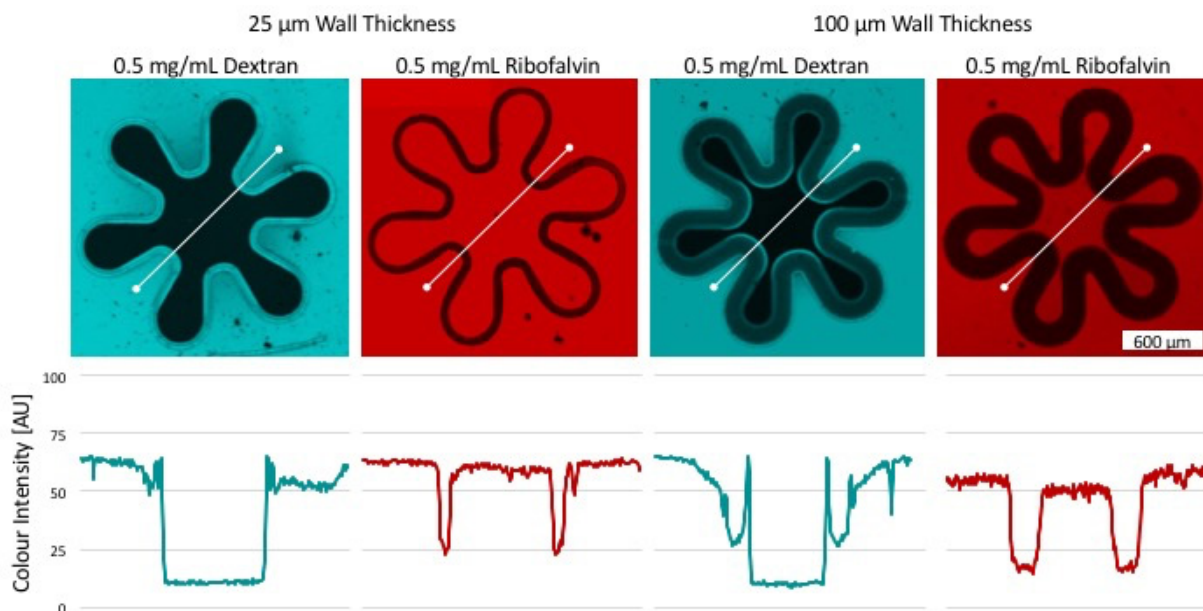


**Figure 6.** Color gradient of riboflavin and dextran shows permeability of the membrane with different wall thicknesses. The color intensity was depicted along a linear axis (white). Thereby the color intensity (AU) of pixels on this line was measured and plotted using the ZEN software. Thereby two different wall thicknesses were analyzed. 25  $\mu\text{m}$  on the left side and 100  $\mu\text{m}$  on the right side. The potential to retain high molecular weight substances was demonstrated using dextran (blue) as in both samples the inner fluorescence signal is approaching zero. Riboflavin (red) on the other side is a membrane permeable substance, shown by equal color intensity within and outside the villous structure.

sides, while dextran stayed exclusively outside of the membrane. Direct comparison of signal differences between inner and outer region numerical values, indicate a marginally improved diffusion capacity of riboflavin in samples with smaller wall thickness. 25  $\mu\text{m}$  samples can be recognized by a significant smaller transition zone compared to 100  $\mu\text{m}$  villi-samples. Here again the dextran signal was detected exclusively outside of the structure while riboflavin levels can be considered equal on both sides. In the range of thickness and 2PP parameters used in this study, no substantial dependence of diffusion was observed.

### 3.6 GelMOD-AEMA Membrane Supports Cell Layer Formation

After the establishment of optimal structuring parameters, material composition and cultivation conditions, membranes were printed followed by seeding with HUVECs and BeWo B30 cells successively. Seeded chips were connected to the microfluidic pump after 24 hours of cell settling, to gain preliminary results about the biocompatibility of the model. For cultivation, the respective channel was supplied with cell type specific media. After 7 days of cultivation under constant flow, the cell layer formation was determined. Therefore, cells were stained with Calcein-AM and imaged using a confocal microscope. The image depicted in Figure 7A shows a three-dimensional view of one loop of the

GelMOD-AEMA membrane, where cells adhered to the channel wall as well as to the chip material. The green tint of the membrane is a result of the high fluorescence of the structured material. The cell layer around the membranous structure is even denser 7 days after seeding, which can be seen in Figure 7B. When enlarged it becomes clear that imaged cells are in different layers, as some of them are more blurred than others (Figure 7C).

## 4. Discussion

The necessity of reliable *in vitro* models in the field of placental research is well reflected by the fact that contradictory data can be found in literature<sup>[17–19,20,21]</sup>. Underlying processes are difficult to study since this transient organ undergoes constant changes, as it controls its own growth and functionality at the same time<sup>[3,17]</sup>. Constantly changing structural arrangement, size, and surface area pose high demands on the model and require a large degree of flexibility. For the simulation of placental processes *in vitro*, not only the material biocompatibility but also high adaptability play a role, as the placental geometry changes during pregnancy.

The usage of microfluidic devices in combination with 2PP techniques offers a complete new range of possibilities. Microfluidic setups mimicking entire organs or organisms are gaining more and more acceptance in the field of tissue engineering and especially in placenta



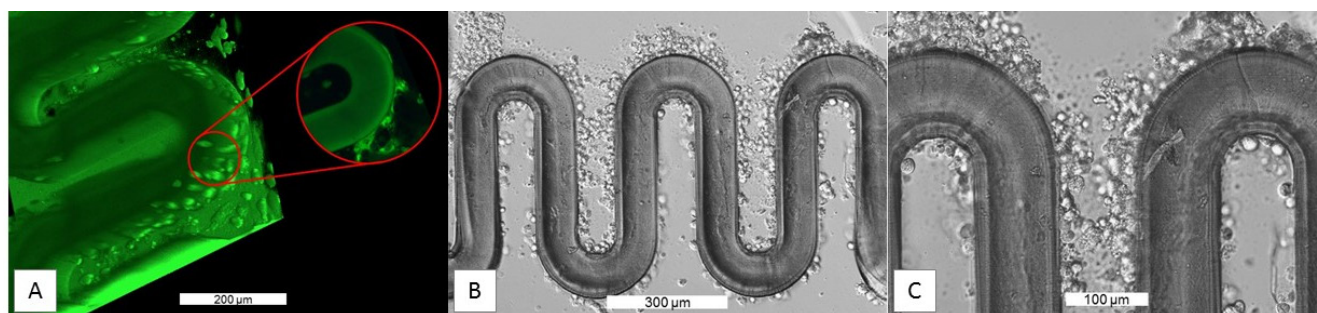


**Figure 7.** Cell Layer adhered to the walls of a GelMOD-AEMA placental membrane. (A) Fluorescence images show the cell layer formation of HUVEC on the membrane wall. The image enlargement on the right side shows a two-dimensional image of HUVECs growing on the channel wall. Furthermore, BeWo B30 cells were recognized on the other side of the membrane. (B) Light microscope images taken after 7 days of incubation clearly show a continuous dense cell layer. (C) In the enlargement, it becomes clear that cells are attached to the membrane at different heights, which is demonstrated by the fact that cells out of focus appear blurry.

research. Therefore, flow profiles of the maternal and fetal blood, and its changes in course of the pregnancy, have to be considered<sup>[1,3,22,23]</sup>.

In this study, three-dimensional geometries within a microfluidic channel were produced from a gelatin-based hydrogel material, mimicking the basal membrane of the placenta. Gelatin, used as substrate or scaffold material, is reported in various studies in the field of tissue engineering<sup>[24–27]</sup>. The material used in this study was a methacrylamide- and methacrylate-modified gelatin hydrogel. GelMOD is reported to be applicable for cell based experiments, as polymerized GelMOD mimics the cellular microenvironment and thus favors the cell attachment and proliferation<sup>[8,10,28]</sup>. Preliminary biocompatibility experiments have shown a slight decrease in viable cell count when cells were plated on GelMOD-AEMA only, but this drawback was successfully tackled by using fibronectin coatings. The improved proliferation of both cells can be explained by the fact that the extra cellular matrix (ECM) proteins gelatin and fibronectin promote cell adhesion and spreading<sup>[29]</sup>. Several studies have shown that fibronectin plays a predominant role in adhesion processes, to neighboring cells as well as to substrate material, in various cell types<sup>[30–33]</sup>. The coating layer facilitates the attachment of the cell as the applied fibronectin can firmly bind to fibronectin deposits in the ECM<sup>[33]</sup>.

The photosensitive gelatin material was polymerized induced by two-photon absorption of precisely focused laser irradiation. Photo-induced crosslinking was thereby depending on the presence of photoinitiators. One of the demands placed on this compound was its water solubility. Sodium dipropanoate-based P2CK fulfills this requirement and proved to be efficient in material formulations containing up to 90% water<sup>[36]</sup>. The x-shaped cultivation chamber not only facilitates the addition of the viscous material GelMOD-AEMA but also allows the separate perfusion of the two generated culture channels, allowing for instance the simulation

of maternal high blood pressure *in vitro*. The chip molds were made of a PEGdma hydrogel. The main advantage of using this material is its permeability. After chip finalization, components of the structure material diffused into the mold material. This feature guarantees a seamless transition between mold and structure material. Furthermore, the attachment of the membrane to the cover and bottom glass surfaces was ensured through their methacrylation *via* silanization. This pretreatment step was performed, as silanization of glass surfaces is known to improve the adhesion properties of polymer materials by covalent bonding<sup>[11]</sup>. The complete sealing of the membrane resulted in two separated cultivation channels. As a consequence, the two different compartments of the placental interface were mimicked. This is also important to make the model visible for the use in transportation studies later on, as it is a prerequisite to guarantee that changes are due to active cell transport and not leakage at connections points. The complete tightness of the membrane, and thus its adhesion to the bottom and cover material as well as its connection to the mold, was verified with a large molecular weight dextran solution. Membrane permeability to sugar-sized substances was demonstrated with riboflavin. Fluorescence intensity analysis confirmed the selective transport of small molecules across the membrane in a time-dependent manner. We proved that measured diffusion of nutrient in subsequent experiments is only dependent on the semi-permeable properties of the membrane and not a result of leakages in the construct itself. Thereby, the barrier thickness in the tested range does not noticeably influence the diffusion behavior.

The barrier model with its two separated channels has the advantage that two cell types can be cultivated in their respective cell culture media at the same time. Nevertheless, diffusion and mixing of media components through the membrane may take place. Therefore, the effect of mixed media, here termed co-culture media,

was investigated. The cultivation of HUVECs in co-culture media showed increased proliferation after 24 and 48 hours, compared to the control. This justifies the conclusion that serum concentrations slightly above those in EGM-2 seem to enhance cell proliferation but does not negatively influence cell viability<sup>[37]</sup>. First tests with the established placenta-on-a-chip model have shown that cell attachment and the formation of a confluent cell layer on the walls of GelMOD-AEMA constructs was feasible. Both cells types, HUVEC and BeWo B30, were successfully seeded and cultured on the membrane walls for 7 days. Our future studies will include optimization of cell seeding conditions and investigation of active glucose transport through the membrane.

## 5. Conclusions

In conclusion, 2PP is an enabling manufacturing technology for establishing a versatile biomimetic on-chip barrier structure suitable for the cultivation of two different cell populations. In this work, collagen derived biopolymers, which resemble the extracellular matrix were applied instead of inorganic polymers. The compatibility of the microfabricated device with microfluidic pumps enables its maintenance under constant flow and thus the simulation of *in vivo* body fluid flow. Customized chip design and channel orientation thereby guarantee the tight separation of the culture compartments, with the advantage that the respective cell type stays in the intended compartment and can be cultivated in its cell culture media. Modified material composition in combination with established structure parameters can be used to produce a selectively permeable membrane, enabling the investigation of complex transport processes for instance. Furthermore, the material supports cell adhesion and monolayer formation of trophoblastic and endothelial cells *in vitro*.

The model reported in this manuscript contributes to the ongoing trend of miniaturization and is the basis for further cell studies as it opens the possibility to investigate the effect of metabolic diseases and blood pressure variations, on the nutrient transportation across the placental barrier. For the simulation of mother's diabetes mellitus, high glucose media will be pumped through the maternal compartment. The implications on the fetal supply can be investigated by measuring glucose concentrations in the collected supernatant using glucose analyzers. Furthermore, the microfluidic model offers the opportunity to investigate the effect of high blood pressure on glucose transport more closely by adapting the pumping speed. Besides the application as a placental model, approaches investigating the barrier function of other tissue layers are conceivable, as this technique can be used to mimic very complex tissue

structures.

Another advantage of this model lies in the adaptability of the geometry. The *in vitro* model has to reflect changes in surface area of the placenta, occurring during the course of pregnancy<sup>[3]</sup>. The use of the 2PP technique using CAD models allows precise structural adaptability of the certain geometry depending on the investigated stage of pregnancy. To this end, surface area can be increased or reduced by addition or removal of villous loops, respectively.

## Conflicts of Interest

There are no conflicts to declare.

## Acknowledgements

The financial support by the FWO Flanders (FWO SB PhD grant, J.V.H.), the Austrian Science Funds (FWF Project No. I2444-N28, A.O.) as well as the European Union's Horizon 2020 research and innovation program (grant agreement No. 685817) and European Research Council (Starting Grant-307701, A.O.) is gratefully acknowledged. Furthermore, we thank the team of the material science and technology department as well as our colleagues from the institute of applied synthetic chemistry at the Technical University of Vienna, for their support and critical comments that greatly improved this work. The authors thank Dr. Tina Buerki-Thurnherr (EMPA, Switzerland) for providing BeWo B30 cells.

## References

1. Lee J S, Romero R, Han Y M, *et al.*, 2015, Placenta-on-a-chip: A novel platform to study the biology of the human placenta. *J Matern Neonatal Med*, 29(7): 1046–1054. <http://dx.doi.org/10.3109/14767058.2015.1038518>
2. Ren K, Zhou J, Wu H, 2013, Materials for microfluidic chip fabrication. *Acc Chem Res*, 46(11): 2396–2406. <http://dx.doi.org/10.1021/ar300314s>
3. Blundell C, Tess E R, Schanzer A S R, *et al.*, 2016, A microphysiological model of the human placental barrier. *Lab Chip*, 16(16): 3065–3073. <http://dx.doi.org/10.1039/c6lc00259e>
4. Sakolish C M, Esch M B, Hickman J J, *et al.*, 2016, Modeling barrier tissues in vitro: Methods, achievements, and challenges. *EBioMedicine*, 5(C): 30–39. <http://dx.doi.org/10.1016/j.ebiom.2016.02.023>
5. Djagny K B, Wang Z, Xu S, *et al.*, 2001, Gelatin: A valuable protein for food and pharmaceutical industries. *Crit Rev Food Sci Nutr*, 41(6): 481–492. <http://dx.doi.org/10.1080/20014091091904>
6. Peinemann K V, Nunes S P, 2007, Application of

- membranes in tissue engineering and biohybrid organ technology. Membrane technology: Membranes for life sciences, 1<sup>st</sup> edition, pp. 343, 2007. <http://dx.doi.org/10.1002/9783527631360.ch8>
7. Van Den Bulcke A I, Bogdanov B, De Rooze N, et al., 2000, Structural and rheological properties of methacrylamide modified gelatin hydrogels. *Biomacromolecules*, 1(1): 31–38. <http://dx.doi.org/10.1021/bm990017d>
  8. Ovsianikov A, Mironov V, Stampfl J, et al., 2012, Engineering 3D cell-culture matrices: Multiphoton processing technologies for biological & tissue engineering applications. *Expert Rev Med Devices*, 9(6): 613–633. <http://dx.doi.org/10.1586/erd.12.48>
  9. Hölzl K, Lin S, Tytgat L, et al., 2016, Bioink properties before, during and after 3D bioprinting. *Biofabrication*, 8(3): 032002. <http://dx.doi.org/10.1088/1758-5090/8/3/032002>
  10. Van Hoorick J, Gruber P, Markovic M, et al., 2017, Cross-linkable gelatins with superior mechanical properties through carboxylic acid modification: Increasing the two-photon polymerization potential. *Biomacromolecules*, 18(10): 3260–3272. <http://dx.doi.org/10.1021/acs.biomac.7b00905>
  11. Tayalia P, Mendonca C R, Baldacchini T, et al., 2008, 3D cell-migration studies using two-photon engineered polymer scaffolds. *Adv Mater*, 20(23): 4494–4498. <http://dx.doi.org/10.1002/adma.200801319>
  12. Paz V F, Emons M, Obata K, et al., 2012, Development of functional sub-100 nm structures with 3D two-photon polymerization technique and optical methods for characterization. *J Laser Appl*, 24(4): 293–301. <http://dx.doi.org/10.2351/1.4712151>
  13. Stampfl J, Liska R, Ovsinikov A, 2016, Multiphoton lithography: Techniques, materials, and applications. in Stampfl J, Liska R, Ovsinikov A, (Eds.) John Wiley & Sons, ISBN: 978-3-527-33717-0
  14. Markovic M, Van Hoorick J, Hölzl K, et al., 2015, Hybrid tissue engineering scaffolds by combination of three-dimensional printing and cell photoencapsulation. *J Nanotechnol Eng Med*, 6(2): 0210011–210017. <http://dx.doi.org/10.1115/1.4031466>
  15. Ovsianikov A, Muehleder S, Torgersen T, et al., 2014, Laser photofabrication of cell-containing hydrogel constructs. *Langmuir*, 30(13): 3787–3794. <http://dx.doi.org/10.1021/la402346z>
  16. Faller A, Schünke M, Schünke G, et al., 2012, Fortpflanzung, Entwicklung und Geburt [in German]. Reproduction, development and birth. in *Der Körper des Menschen*, Stuttgart: Georg Thieme Verlag, 16<sup>th</sup> edition, pp. 752ff, 2012.
  17. Desoye G, Gauster M, Wadsack C, et al., 2011, Placental transport in pregnancy pathologies. *Am J Clin Nutr*, 94(6): 1896–1902. <http://dx.doi.org/10.3945/ajcn.110.000851>
  18. Gallo L A, Barrett H L, Dekker N M, 2016, Review: Placental transport and metabolism of energy substrates in maternal obesity and diabetes. *Placenta*, 54: 59–67. <http://dx.doi.org/10.1016/j.placenta.2016.12.006>
  19. Gaccioli F, Lager S, Powell T L, et al., 2012, Placental transport in response to altered maternal nutrition. *J Dev Orig Health Dis*, 4(2): 1–15. <http://dx.doi.org/10.1017/S2040174412000529>
  20. Gaither K, Quraishi A N, Illsley N P, 2016, Diabetes alters the expression and activity of the human placental GLUT1 glucose transporter. *J Clin Endocrinol Metab*, 84(2): 695–701. <http://dx.doi.org/10.1210/jcem.84.2.5438>
  21. Jansson T, Ekstrand Y, Wennergren M, et al., 2001, Placental glucose transport in gestational diabetes mellitus. *Am J Obstet Gynecol*, 184(2): 111–116. <http://dx.doi.org/10.1067/mob.2001.108075>
  22. Miura S, Sato K, Kato-Negishi M, et al., 2015, Fluid shear triggers microvilli formation via mechanosensitive activation of TRPV6. *Nat Commun*, 6(12): 8871. <http://dx.doi.org/10.1038/ncomms9871>
  23. Caplin J D, 2016, Utilizing microfluidic technology to replicate placental functions in a drug testing model. 2016. Global Congress on NanoEngineering for Medicine and Biology.
  24. Chen S, Zhang Q, Nakamoto T, et al., 2016, Gelatin scaffolds with controlled pore structure and mechanical property for cartilage tissue engineering. *Tissue Eng Part C Methods*, 22(3): 189–198.
  25. Gorgieva S, Kokol V, 2011, Biomaterials and their biocompatibility: Review and perspectives. *InTech*, 1–36.
  26. Markovic M, Van Hoorick J, Hölzl K, et al., 2015, Hybrid tissue engineering scaffolds by combination of three-dimensional printing and cell photoencapsulation. *J Nanotechnol Eng Med*, 6(2): 1–7. <http://dx.doi.org/10.1115/1.4031466>
  27. Van Hoorick J, Gruber P, Markovic M, et al., 2018, Highly reactive thiol-norbornene photo-click hydrogels: Toward improved processability. *Macromolecular Rapid Commun*: 1800181, <http://dx.doi.org/10.1002/marc.201800181>
  28. Nichol J W, Koshy S T, Bae H, et al., 2010, Cell-laden microengineered gelatin methacrylate hydrogels. *Biomaterials*, 31(21): 5536–5544. <http://dx.doi.org/10.1016/>

- j.biomaterials.2010.03.064
29. Maquoi E, Noel A, Foidart J M, 1997, Matrix metalloproteinases in choriocarcinoma cell lines: A potential regulatory role of extracellular matrix components. in *Placental Molecules in Hemodynamics, Transport, and Cellular Regulation*, T. Hata, M. Takayama, I. Taki, and J.-M. Foidart, pp. 585, 1997.
  30. Ruoslahti E, Pierschbacher M D, 1987, New perspectives in cell adhesion: RGD and integrins. *Am Assoc Adv Sci*, 238(4826): 491–497. <http://dx.doi.org/10.1126/science.2821619>
  31. PeproTech, 2014, Endothelial cell media-maintenance media for endothelial cells.
  32. Seeger J M, Klingman N, *et al.*, 1985, Improved endothelial cell seeding with cultured cells and fibronectin-coated grafts. *J Surg Res*, 38(6): 641–647.
  33. Ruoslahti E, 1984, Fibronectin in cell adhesion and invasion. *Cancer Metastasis Rev*, 3(1): 43–51.
  34. Wang Q, 2017, Fabrication of photo-mediated biomaterial scaffolds. in *Smart Materials for Tissue Engineering: Fundamental Principles*, Q. Wang, Ed. 2017.
  35. Ren K, Zhou J, Wu H, 2013, Materials for microfluidic chip fabrication. *Acc Chem Res*, 46(11): 2396–2406. <https://dx.doi.org/10.1021/ar300314s>
  36. Dendukuri D, Panda P, Haghgoie R, *et al.*, 2008, Modeling of oxygen-inhibited free radical photopolymerization in a PDMS microfluidic device. *Macromolecules*, 41(22): 8547–8556.
  37. Altannavch T S, Roubalová K, Era P K U Č, 2004, Effect of high glucose concentrations on expression of ELAM-1, VCAM-1 and ICAM-1 in HUVEC with and without cytokine activation. *Physiol Res*, 53: 77–82. Available from: <http://citeseerx.ist.psu.edu/viewdoc/download?doi=10.1.1.655.1274&rep=rep1&type=pdf>